Phys. kondens. Materie 6, 206–217 (1967)

Single-particle Spectrum of the Degenerate Electron Gas

II. Numerical Results for Electrons Coupled to Plasmons *

B. I. LUNDQVIST
Institute of Theoretical Physics, Sven Hultins gata, Göteborg, Sweden

Received March 10, 1967

The single-particle spectrum of an interacting electron gas is investigated in an approximation with electrons coupled to plasmons. Extensive numerical results for the spectral weight function, the momentum distribution function and the density of states are presented over a range of metallic densities.

On examine le spectre à une particule d'un gaz d'électrons interagissants, dans le cadre d'une approximation faisant intervenir le couplage des électrons et des plasmons. On présente de nombreux résultats numériques concernant la densité spectrale, la fonction de distribution d'impulsion et la densité d'états dans un certain domaine de densités métalliques.

Das Einteilchenspektrum eines wechselwirkenden Elektronengases wird in einer Näherung untersucht, welche die Kopplung zwischen Elektronen und Plasmonen berücksichtigt. Es werden für einen Bereich von metallischen Dichten umfassende numerische Ergebnisse für die spektrale Gewichtsfunktion, die Impulsverteilungsfunktion und die Zustandsdichte angegeben.

I. Introduction

In a preceding paper [1] it was shown that the singular Coulomb potential and the plasmon pole of the effective interaction give rise to a characteristic structure in the single-particle spectral weight function. For electron momenta smaller than a critical value a new pole of the one-electron Green function appears on the real axis, representing a new elementary mode. When higher order terms are included, this pole will move off the real axis, but a strong resonance is still expected to occur.

In this paper those conclusions are illustrated in a particular model, in which a simple interpolation formula for the dielectric function has been used, and which involves the main features of the Random Phase Approximation (RPA). It is shown that the new elementary excitation, a coupled mode of plasmon-hole states, has an appreciable spectral weight at metallic densities. The density of states is drastically changed by the interaction. The main parabolic band is reduced, and there is a new band below the main band. In the bottom of this sideband there is a peak due to the plasmon-hole states.

An expression for the electron self-energy in the lowest order approximation is given in Section II. Numerical results concerning the quasiparticle properties, the total energy and the specific heat are compared with earlier calculations in Section III, and in the following section extensive numerical results for the spectral weight function, the momentum distribution function and the density of

* Partially supported by the Swedish Atomic and Natural Science Research Councils.

states are presented for a range of electron densities. The paper is finished off with some remarks in Section V.

II. An Approximation for the Self-energy

In part I the self-energy of an electron in an interacting electron gas has been analysed. The main effect studied comes from the coupling between the electron and the plasmon resonance. Therefore the self-energy may be written as a sum of the Hartree-Fock expression and the self-energy due to coupling to the plasmon field,

$$M(k, \mathscr{E}) = M_{\mathrm{HF}}(k) + i\hbar \int \frac{d^4q}{(2\pi)^4} |g_q|^2 \frac{2\omega_q}{\omega^2 - \omega_q^2 + i\delta} \times \times \frac{1}{\mathscr{E} - \omega - \mathscr{E}(\boldsymbol{k} - \boldsymbol{q}) - \mathscr{E}_0 + i(k_{\mathrm{F}} - |\boldsymbol{k} - \boldsymbol{q}|)\delta}, \tag{1}$$

where M_{HF} is the Hartree-Fock exchange potential

$$M_{\mathrm{HF}}(k) = -\frac{\hbar^2 k_{\mathrm{F}}}{\pi m a_0}\left(1 + \frac{k_{\mathrm{F}}^2 - k^2}{2kk_{\mathrm{F}}} \ln\left|\frac{k_{\mathrm{F}} + k}{k_{\mathrm{F}} - k}\right|\right). \tag{2}$$

The notations are explained in part I. The shift in the chemical potential,

$$\mathscr{E}_0 = \mu - \mathscr{E}(k_{\mathrm{F}}), \tag{3}$$

is given by [2]

$$\mathscr{E}_0 = M_0(k_{\mathrm{F}}, \mathscr{E}(k_{\mathrm{F}})), \tag{4}$$

where

$$M_0(k, \mathscr{E}) = M(k, \mathscr{E} + \mathscr{E}_0). \tag{5}$$

The electron-plasmon coupling constant is [3]

$$|g_q|^2 = \frac{e^2\omega_{\mathrm{p}}^2}{2\varepsilon_0\omega_q} \cdot \frac{1}{q^2}, \tag{6}$$

and the plasmon dispersion law is taken as

$$\omega_q^2 = \omega_{\mathrm{p}}^2 + v_{\mathrm{F}}^2 q^2/3 + (\hbar q^2/2m)^2, \tag{7}$$

where $\omega_{\mathrm{p}} = \sqrt{ne^2/(\varepsilon_0 m)}$ is the plasma frequency and $v_{\mathrm{F}} = \hbar k_{\mathrm{F}}/m$ the Fermi velocity.

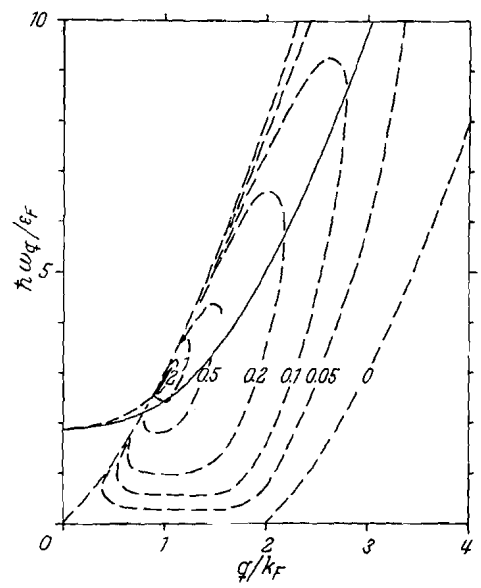

Fig. 1. The dispersion curve (solid) according to Eq. (7) compared to the RPA density-fluctuation spectrum at $r_s = 4$. The dotted curve is the RPA plasmon energy, and the level curves give the values of $\mathrm{Im}(1/\varepsilon_{\mathrm{RPA}})$

The plasmon is assumed to be welldefined for all momenta. As can be seen from Fig. 1, the dispersion law in Eq. (7) follows rather closely the RPA plasmon dispersion law and at short wavelengths the maximum of the RPA spectral weight function for the density fluctuations, $\mathrm{Im}(1/\varepsilon_{\mathrm{RPA}})$.

The coefficient in front of the q^2-term in Eq. (7) is a factor 5/9 smaller than the RPA coefficient. It is chosen so as to give the Thomas-Fermi potential

$$v_q/\varepsilon(\boldsymbol{q}, 0) \to 1/\varepsilon_0(q^2 + k_{\mathrm{TF}}^2) \tag{8}$$

in the static long wavelength limit, $k_{TF} = \sqrt{3}\omega_p/v_F$ being the Thomas-Fermi screening constant. The resulting self-energy does not depend sensitively upon the precise value of the q^2-coefficient in the dispersion law. The q^4-term in Eq. (7) is however very important, determing the contributions from short wavelength fluctuations.

The dielectric function

$$\varepsilon(\boldsymbol{q}, \omega) = (\omega_q^2 - \omega^2)/(\omega_q^2 - \omega_p^2 - \omega^2) \tag{9}$$

corresponding to the approximation in Eq. (1) fulfils the sum rules

$$\int_0^\infty d\omega\, \omega\, \mathrm{Im}\{1/\varepsilon(\boldsymbol{q}, \omega + i\delta)\} = -\frac{\pi}{2}\omega_p^2 \tag{10}$$

and

$$\int_0^\infty d\omega\, \omega\, \mathrm{Im}\{\varepsilon(\boldsymbol{q}, \omega + i\delta)\} = \frac{\pi}{2}\omega_p^2. \tag{11}$$

This approximate dielectric function serves as a convenient interpolation formula, which in an integral expression like Eq. (1) reproduces the main features of the full density fluctuation propagator. The main approximation comes from the neglect of the particle-hole continuum. Therefore there will be no damping of the quasiparticle in the region of small momenta, where damping due to excitation of particle-hole pairs is the important mechanism. Equation (1) thus gives a sharp quasiparticle peak with windows in the spectrum on both sides for electrons not too far from the Fermi surface. This work is mainly concerned with the properties at frequencies where plasmon excitation is the dominant mechanism, and there Eq. (1) gives a good description.

The ω-integration in Eq. (1) is performed by closing the integration contour and picking up the contributions from the plasmon and hole poles. Letting $\delta' \to 0$, the expression becomes

$$M_0(k, \mathscr{E}) = M_{HF}(k) + \frac{\hbar}{(2\pi)^2 k}\int_0^\infty q\,dq\,|g_q|^2 \int_{|k-q|}^{k+q} p\,dp \times \\ \times \left[\frac{\Theta(k_F - p)}{\mathscr{E} - \mathscr{E}(p) + \hbar\omega_q - i\delta} + \frac{\Theta(p - k_F)}{\mathscr{E} - \mathscr{E}(p) - \hbar\omega_q + i\delta}\right]. \tag{12}$$

By performing the p-integrations, Eq. (12) may be expressed as a sum of one-dimensional integrals,

$$M_0(k, \mathscr{E}) = M_{HF}(k) - \frac{\hbar\omega_p^2}{2\pi a_0 k} \times \tag{13}$$

$$\times \left\{\int_{k+k_F}^\infty \frac{dq}{q\omega_q}\left[\ln\left|\frac{\mathscr{E}(k+q) - \mathscr{E} + \hbar\omega_q}{\mathscr{E}(k-q) - \mathscr{E} + \hbar\omega_q}\right| - \pi i\,\Theta(\mathscr{E}(k+q) - \mathscr{E} + \right.\right.$$

$$+ \hbar\omega_q)\,\Theta(\mathscr{E} - \hbar\omega_q - \mathscr{E}(k-q))\Big] + \int_{|k_F-k|}^{k+k_F} \frac{dq}{q\omega_q}\left[\ln\left|\frac{\mathscr{E}(k_F) - \mathscr{E} - \hbar\omega_q}{\mathscr{E}(k-q) - \mathscr{E} - \hbar\omega_q}\right| \times\right.$$

$$\times \frac{\mathscr{E}(k+q) - \mathscr{E} + \hbar\omega_q}{\mathscr{E}(k_F) - \mathscr{E} + \hbar\omega_q}\Big| + \pi i\,\Theta(\mathscr{E}(k_F) - \mathscr{E} - \hbar\omega_q)\,\Theta(\mathscr{E} + \hbar\omega_q -$$

$$\left.\left. - \mathscr{E}(k-q)) - \pi i\,\Theta(\mathscr{E}(k+q) - \mathscr{E} + \hbar\omega_q)\,\Theta(\mathscr{E} - \hbar\omega_q - \mathscr{E}(k_F))\right] +\right.$$

$$+\Theta(k_F-k)\int_0^{k_F-k}\frac{dq}{q\,\omega_q}\left[\ln\left|\frac{\mathscr{E}(k+q)-\mathscr{E}-\hbar\omega_q}{\mathscr{E}(k-q)-\mathscr{E}-\hbar\omega_q}\right|+\right.$$

$$\left.+\pi i\,\Theta(\mathscr{E}(k+q)-\mathscr{E}-\hbar\omega_q)\,\Theta(\mathscr{E}+\hbar\omega_q-\mathscr{E}(k-q))\right]+$$

$$+\Theta(k-k_F)\int_0^{k-k_F}\frac{dq}{q\,\omega_q}\left[\ln\left|\frac{\mathscr{E}(k+q)-\mathscr{E}+\hbar\omega_q}{\mathscr{E}(k-q)-\mathscr{E}+\hbar\omega_q}\right|-\pi i\,\Theta(\mathscr{E}(k+q)-\mathscr{E}+\right.$$

$$\left.\left.+\hbar\omega_q)\,\Theta(\mathscr{E}-\hbar\omega_q-\mathscr{E}(k-q))\right]\right\}.$$

These integrals have been computed numerically on a CD 3600 computer using algorithms for adaptive Simpson integration [4] and for zeros of arbitrary function [5].

III. Quasiparticle Properties, Total Energy and Specific Heat

To check the usefulness of the interpolation formulation (Eq. (9)) for the dieleetric function comparisons with earlier results calculated in the same approximation but with the full Lindhard dielectric function have been made.

Table 1. *The chemical potential* $\mu = \mathscr{E}(k_F) + \mathscr{E}_0$ *for an electron gas with* $\mathscr{E}_0 = M_0(k_F, \mathscr{E}(k_F))$ *according to Eq.* (4) *compared to the* RPA-*values* ([2]). *Energies are given in rydbergs* (1 Ry = 13.6 eV)

r_s	$\mathscr{E}(k_F)$ Ry	$\mathscr{E}_0$ Eq. (4) Ry	RPA Ry	r_s	$\mathscr{E}(k_F)$ Ry	$\mathscr{E}_0$ Eq. (4) Ry	RPA Ry
1	3.6832	− 1.382	− 1.3965	6	0.1023	− 0.286	− 0.2926
2	0.9208	− 0.738	− 0.7491	7	0.0752	− 0.252	− 0.2575
3	0.4092	− 0.516	− 0.5259	8	0.0576	− 0.226	− 0.2308
4	0.2302	− 0.403	− 0.4112	9	0.0455	− 0.205	− 0.2097
5	0.1473	− 0.333	− 0.3406	10	0.0368	− 0.188	− 0.1925

In Table 1 it is shown that the chemical potential μ for a range of r_s-values agrees within 2.5 percent with the RPA-results ($3/4\pi(r_s a_0)^3$ = electron density).

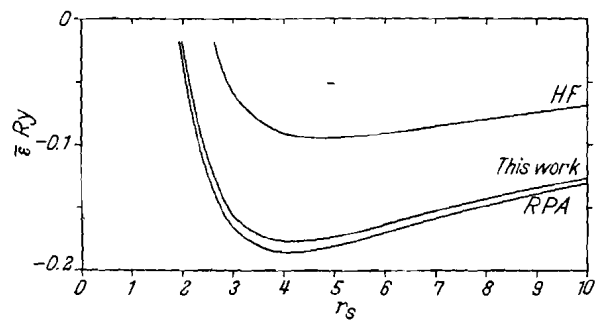

Fig. 2. Total energy of the electron gas according to Eq. (14) compared to the Hartree-Fock (HF) and RPA results taken from [2]

The total energy per particle, $\overline{\mathscr{E}}$, is given by the chemical potential according to the formula [6]

$$\overline{\mathscr{E}} = 3 r_s^3 \int_{r_s}^{\infty} \frac{\mu(x)}{x^4}\, dx. \tag{14}$$

A comparison with the total RPA energy is made in Fig. 2.

Table 2. *The renormalization constants Z and the energies ω of the quasiparticle* (Q) *and of the new excitation* (pn) *in the undamped regions. Energies are expressed in rydbergs and measured from the Fermi level*

r_s	k/k_F=	0.0	0.2	0.4	0.6	0.8	1.0	1.2	1.4	1.6
1	Z_Q	0.753	0.753	0.761	0.791	0.839	0.877	0.846	0.728	
	ω_Q	− 3.770	− 3.615	− 3.159	− 2.416	− 1.373	0.000	1.663	3.525	
	Z_{pn}	0.205								
	ω_{pn}	− 6.95								
2	Z_Q	0.645	0.650	0.669	0.706	0.755	0.793	0.768	0.704	
	ω_Q	− 0.915	− 0.879	− 0.772	− 0.594	− 0.339	0.000	0.413	0.880	
	Z_{pn}	0.325	0.304							
	ω_{pn}	− 2.626	− 2.590							
3	Z_Q	0.581	0.588	0.610	0.646	0.693	0.728	0.707	0.656	0.545
	ω_Q	− 0.396	− 0.381	− 0.336	− 0.259	− 0.148	0.000	0.181	0.388	0.614
	Z_{pn}	0.367	0.358	0.316						
	ω_{pn}	− 1.407	− 1.392	− 1.350						
4	Z_Q	0.537	0.543	0.565	0.600	0.643	0.676	0.658	0.614	0.537
	ω_Q	− 0.218	− 0.210	− 0.185	− 0.143	− 0.082	0.000	0.101	0.216	0.344
	Z_{pn}	0.397	0.387	0.353						
	ω_{pn}	− 0.918	− 0.907	− 0.875						
5	Z_Q	0.502	0.509	0.529	0.562	0.602	0.632	0.617	0.579	0.517
	ω_Q	− 0.137	− 0.132	− 0.116	− 0.090	− 0.052	0.000	0.064	0.137	0.218
	Z_{pn}	0.418	0.409	0.376	0.271					
	ω_{pn}	− 0.663	− 0.655	− 0.630	− 0.584					
6	Z_Q	0.474	0.481	0.500	0.531	0.567	0.596	0.582	0.548	0.496
	ω_Q	− 0.094	− 0.090	− 0.080	− 0.062	− 0.035	0.000	0.044	0.094	0.151
	Z_{pn}	0.432	0.423	0.392	0.307					
	ω_{pn}	− 0.510	− 0.503	− 0.484	− 0.448					

The quasiparticle parameters, i. e. the renormalization constant

$$Z(k) \cong 1 \Big/ \left(1 - \frac{\partial}{\partial \mathscr{E}} M_0(k, \mathscr{E}(k))\right) \tag{15}$$

and the quasiparticle energy

$$E(k) \cong \mathscr{E}(k) + \mathscr{E}_0 + Z(k)\,(M_0(k, \mathscr{E}(k)) - \mathscr{E}_0) \tag{16}$$

have been computed, and typical results in the regions of no damping are shown in Table 2. Except for the absence of damping there is reasonable agreement with the corresponding RPA-values [2]. In Fig. 3 the discontinuity of the momentum distribution function at the Fermi surface, $Z_F = Z(k_F)$, is shown for several idfferent approximations [2, 7—10]. The result of this paper is only a few percent greater than the RPA-values.

QUINN [11] has published data on the range of excited electrons in an electron gas. The lifetime of the electron is related to the imaginary part of the self-energy at the electron energy [12, 13]. For not too energetic electrons the renormalization gives a correction, and the inverse lifetime becomes two times the imaginary part of the quasiparticle energy,

$$E_2(k) \cong \mathrm{Re}\, Z(k)\, \mathrm{Im}\, M_0(k, \mathscr{E}(k)) + \quad (17)$$
$$+ \mathrm{Im}\, Z(k)\, (\mathrm{Re}\, M_0(k, \mathscr{E}(k)) - \mathscr{E}_0)\,.$$

A comparison with QUINN's results is made in Fig. 4. Of course there is no damping due to pair excitation in Eq. (17), but in the region of plasmon excitation the curves show the same behaviour.

The specific heat calculated according to the formula [14]

$$\frac{C}{C_0} = \frac{d\mathscr{E}(k)}{dk} \Big/ \frac{dE(k)}{dk}\Big|_{k=k_F} \quad (18)$$

is compared in Fig. 5 to the results of other approximations. The corrections to the Sommerfeld value C_0 are smaller than with the RPA and HUBBARD [10] dielectric functions. However, the values are in close agreement with HEDIN's results [2], which include effects up to second order in the effective interaction v_q/ε.

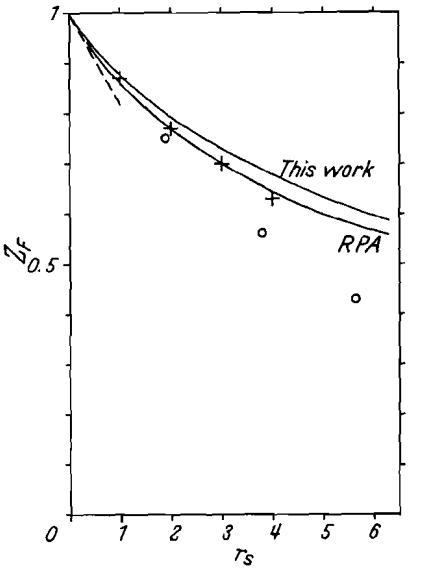

Fig. 3. The renormalization constant for a quasiparticle on the Fermi surface, $Z_F = Z(k_F)$, equal to the discontinuity of the momentum distribution function. The result of this paper is compared with the RPA results according to [2, 7—9] and values obtained with the Hubbard dielectric function (+, [10]) and with exchange corrections (°, [9])

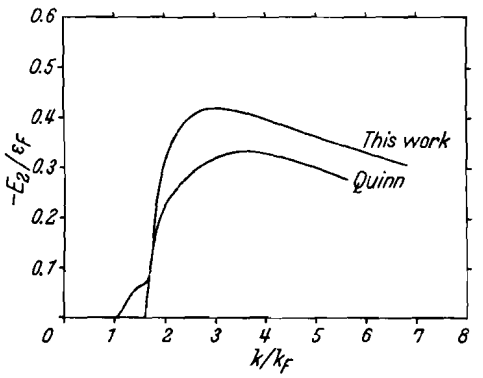

Fig. 4

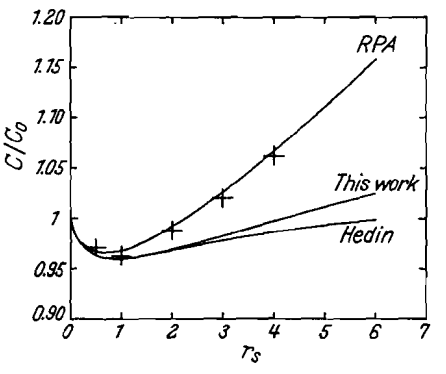

Fig. 5

Fig. 4. The imaginary part of the quasiparticle energy at $r_s = 2$ compared with the results of [11], $\mathscr{E}_F$ being the kinetic energy at the Fermi surface, $\mathscr{E}(k_F)$

Fig. 5. The specific heat compared with the RPA-results (from [2]) and with the values by RICE (+, [10]) and HEDIN [2], C_0 being the Sommerfeld value

These results have been shown in order to get an idea of the accuracy and usefulness of the approximation in Eq. (1) for the self-energy in relation to the use of the RPA dielectric function. Because the theory contains lowest order effects only and thus can be formally justified only in the high density limit, emphasis should be placed mainly on the qualitative features of the results. For an investigation over a range of densities and a large region of momenta and energies, as will be presented in the following section, it is felt that Eq. (1) forms an adequate starting point, with the usual reservation that the results will gradually loose their significance, when going far away from the high density region.

IV. The Spectral Weight Function

The single-particle properties of a system are completely described by the spectral weight function $A(\boldsymbol{k}, \omega)$, which is related to the one-electron propagator $G(\boldsymbol{k}, \mathscr{E})$ according to

$$G(k, \mathscr{E}) = \int_{-\infty}^{\infty} \frac{A(\boldsymbol{k}, \omega)\, d\omega}{\mathscr{E} - \mu - \omega + i\,\delta\omega}. \tag{19}$$

The real and imaginary parts of the self-energy $M(\boldsymbol{k}, \mathscr{E})$ according to Eqs. (5) and (13) have been computed for a range of densities typical for metals, and $A(\boldsymbol{k}, \omega)$ has been calculated from the formula

$$A(\boldsymbol{k}, \omega) = \frac{1}{\pi} \frac{|\operatorname{Im} M(\boldsymbol{k}, \omega + \mu)|}{(\omega + \mu - \mathscr{E}(\boldsymbol{k}) - \operatorname{Re} M(\boldsymbol{k}, \omega + \mu))^2 + (\operatorname{Im} M(\boldsymbol{k}, \omega + \mu))^2}. \tag{20}$$

The (k, ω)-dependence of the spectral weight function is displayed in Figs. 6—8.

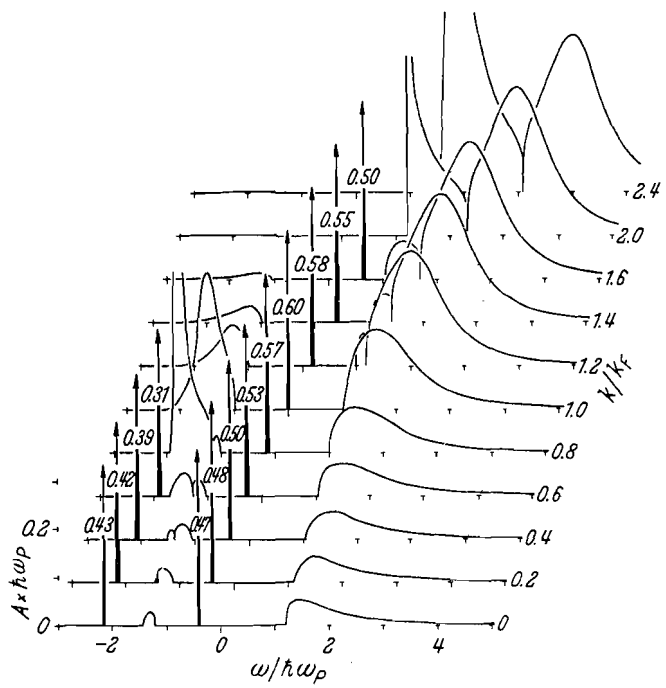

Fig. 6. Typical behaviour of the spectral weight function $A(k, \omega)$. The numbers in the figure give the weights Z of the δ-function peaks. The curves are drawn for $r_s = 6$ ($\hbar\omega_p = 0.236$ Ry)

For positive (negative) energies ω the spectral weight function $A(\boldsymbol{k}, \omega)$ expresses the relative probability per energy unit for the system to be in a state with an energy $\omega + \mu$ $(-\omega - \mu)$ above the ground state just after injection of one electron (hole) of momentum $\boldsymbol{k}$ [15].

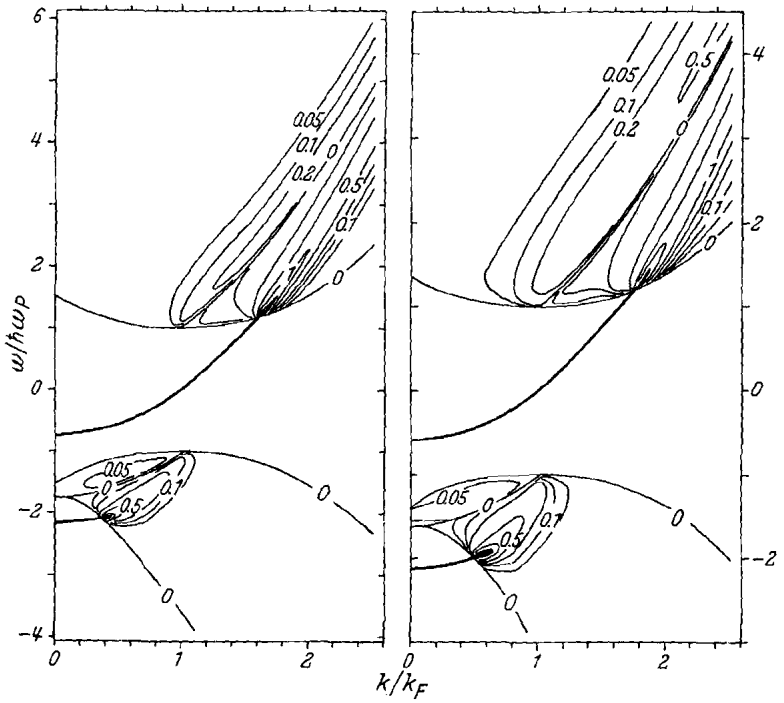

Fig. 7. The spectral weight function $A(k, \omega)$ at $r_s = 2$ and 3, the plasma energy $\hbar\omega_p$ being 1.225 and 0.667 Ry, respectively. The dispersion curves of the two undamped excitations are drawn with heavy lines, and in the regions with damped excitations the values of $A(k, \omega)$ are given by the level curves

As discussed in paper I the spectral weight function consists typically of three components, one singular peak and two sidebands for most values of the momentum $\boldsymbol{k}$ as is seen in Fig. 6. Figures 7 and 8 are extensions of the common plot of the dispersion law $\omega = \mathscr{E}(k) - \mathscr{E}(k_F)$ of the independent-particle model to include the modifications of the spectrum due to the interaction. These figures give the level curves for the spectral weight function $A(k, \omega)$, and the heavy lines show the dispersion laws of the eigenvalues to the $N \pm 1$ electron Hamiltonian. Excitation energies of the $(N-1)$-particle system are measured along the negative ω-axis.

In the electron-plasmon model the eigenvalues exist for momenta not too large (cf. Table 2). As mentioned in Section II there is no damping of the quasiparticle due to excitation of particle-hole pairs because of the approximate dielectric function in Eq. (9). At momenta k large enough to make $\mathscr{E}(k) - \mathscr{E}(k_F) > \hbar\omega_{k-k_F}$ the damping due to plasmon excitations sets in. The critical momentum for the new elementary excitation, which may be called a "plasmaron", is given by the

condition $\omega_{\rm pn}(k) > -\hbar\omega_{k+k_F}$ and increases with increasing r_s-value. The shifts in the quasiparticle energy from the Hartree value $\mathscr{E}(k) - \mathscr{E}(k_F)$ are very small, and the "plasmaron" peak at $\omega_{\rm pn}(k)$ is typically $(1.4-1.7) \times \hbar\omega_p$ to the left of the quasiparticle peak on the ω-axis. Both the quasiparticle and the "plasmaron" have almost quadratic dispersion laws.

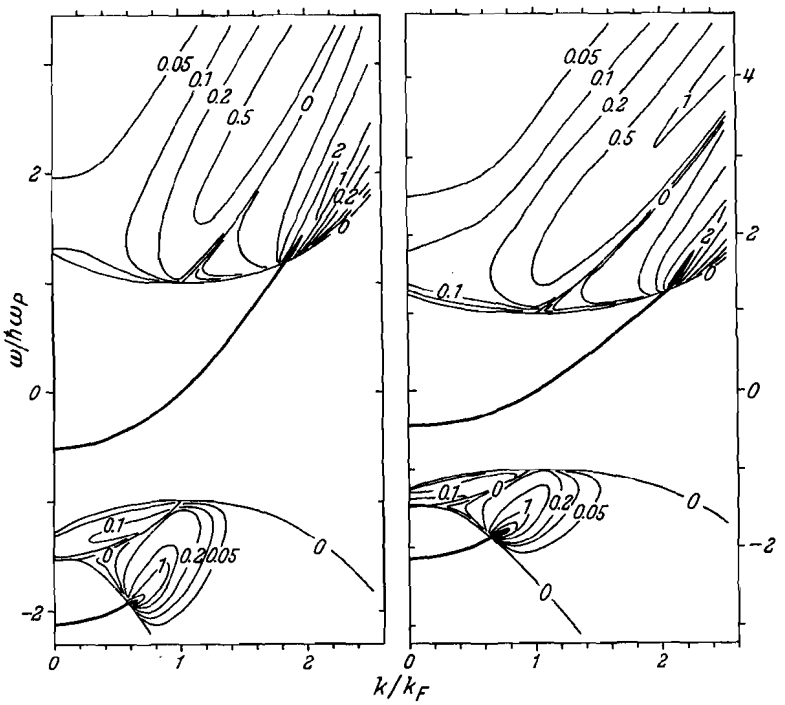

Fig. 8. The spectral weight function $A(k, \omega)$ at $r_s = 4$ and 5 ($\hbar\omega_p = 0.435$ and 0.310 Ry, respectively)

In Fig. 6 and in Table 2 the strengths of the peaks of $A(k, \omega)$ are indicated by the values of the corresponding renormalization constants Z. As in previous calculations [2, 7—10] there is a considerable reduction in the strength of the quasiparticle peak due to the interaction.

The new and interesting result of this calculation is not only the existence of the new excitation but also the appreciable spectral weight, which is associated with it. Near the bottom of the Fermi sea the quasiparticle and the "plasmaron" have almost all of the available spectral weight attached to them, and at metallic densities only 5—10 percent falls into the continuous parts of the single-particle spectrum. At low metallic densities the contributions form the two eigenvalues to the sum rule

$$\int_{-\infty}^{\infty} d\omega\, A(\boldsymbol{k}, \omega) = 1 \tag{21}$$

are almost equal for small k-values.

Even when the "plasmaron" has entered the continuous region, it gives a characteristic contribution to the spectrum. Both for momenta below and above the Fermi surface a broad peak in the spectral weight function is distinguishable from the incoherent contributions to the sidebands. The right (left) sideband covers a large area for k above (below) the Fermi momentum k_F. For instance there is 35 percent probability of exciting the system into energies above $\hbar\omega_{0.4k_F}$, when an electron with momentum $k = 1.4\,k_F$ is added to an electron gas with $r_s = 4$.

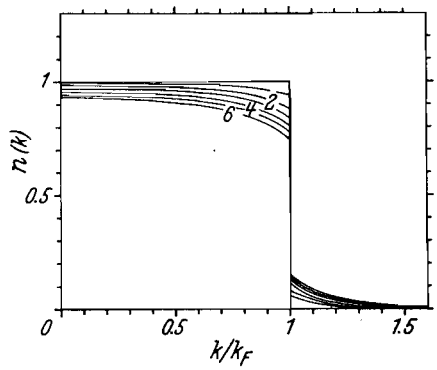

Fig. 9. The momentum distribution function $n(k)$

The sum rule in Eq. (21) has been numerically fulfilled with an error smaller than two percent, which number may be taken as a measure of the numerical accuracy in the calculations.

The momentum distribution function

$$n(\boldsymbol{k}) = \int_{-\infty}^{0} d\omega\, A(\boldsymbol{k}, \omega) \tag{22}$$

is drawn in Fig. 9 for several r_s-values. The curves show that in the ground state also electron states with momenta above the Fermi surface are occupied, and that

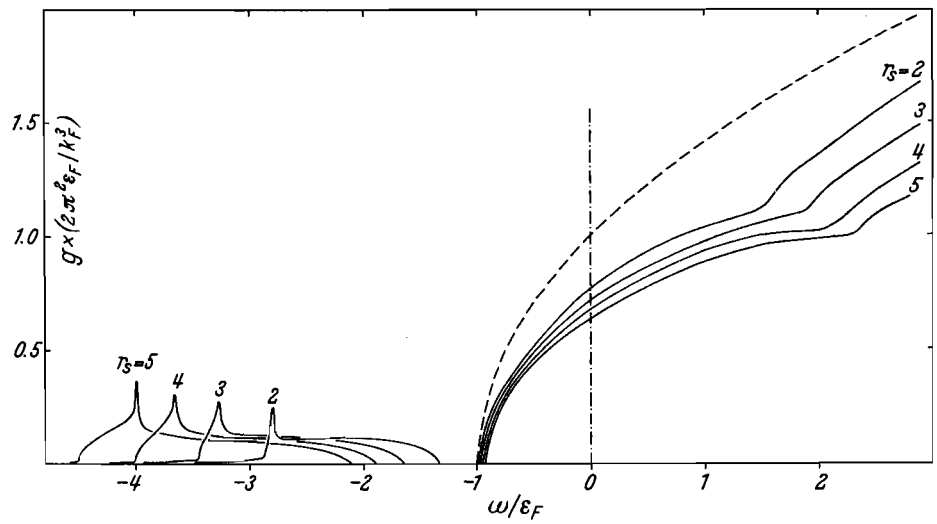

Fig. 10. The density of states $g(\omega)$. The dashed curve is the result of the one-electron theory, and the vertical broken line indicates the Fermi level

even at zero temperature a considerable part of the electron states with momenta smaller than k_F are unoccupied.

In Fig. 10 the density of states

$$g(\omega) = \frac{1}{4\pi^3} \int d^3k\, A(\boldsymbol{k}, \omega) \tag{23}$$

is shown for different electron densities. The dotted curve is the parabola of the one-electron theory. Compared to it, Eq. (23) gives three modifications. The reduced quasiparticle weight $Z(k)$ gives a lower density of states in the main band. There is further a contribution from the right sideband of $A(\boldsymbol{k}, \omega)$, which for energies more than $\hbar\omega_p$ above the Fermi level almost compensates the reduction in the density of states. Finally there is a new band at energies more than $\hbar\omega_p$ below the Fermi surface. The peak in this low-energy band is due to the "plasmaron" states.

V. Concluding Remarks

Calculations of the self-energy of an electron in an interacting electron gas have been presented in a model, where the electron-plasmon coupling has been considered. The resulting single-particle spectrum shows a characteristic structure with the plasma energy $\hbar\omega_p$ being a natural unit for the energy scale. A new elementary excitation, a "plasmaron", undamped in the electron-plasmon model, appears for small electron momentum.

A numerical evaluation of the *imaginary* part of the self-energy $M(\boldsymbol{k}, \mathscr{E})$ in the RPA has been performed recently by BOSE et al. [16]. As the aim of that calculation was only to provide a tabulation for reference purpose, they did not notice the drastic self-energy effects on the single-particle spectrum. If both the real and imaginary parts of $M(\boldsymbol{k}, \mathscr{E})$ are computed in RPA and put into Eq. (20),

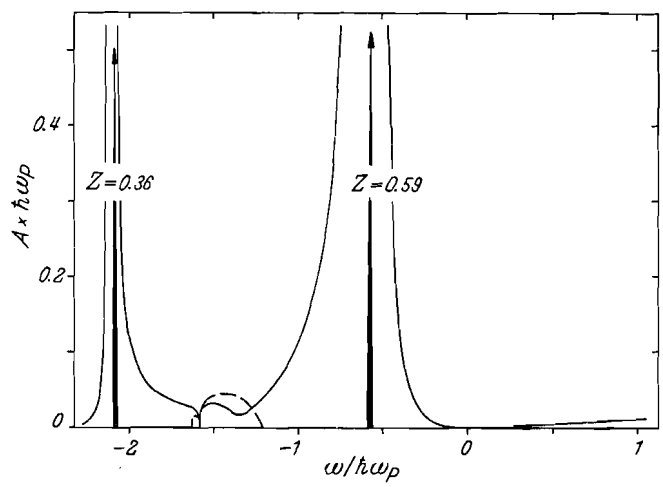

Fig. 11. Typical behaviour of the spectral weight function $A(k, \omega)$ in RPA ($r_s = 3$, $k = 0.2\, k_F$). Comparison is made with the result of this paper, given as a broken curve and two arrowed peaks with weights Z

the spectral weight function $A(\boldsymbol{k}, \omega)$ becomes typically as in Fig. 11. The new excitation remains, very weakly damped, and the only important change of the spectral weight function is as expected the broadening of the quasiparticle peak. Thus the main conclusions of this paper are confirmed in the RPA *.

* A more complete report on results in the RPA will be published separately.

In a second iteration of the Dyson equation, i. e. with the bare propagator in Eq. (1) replaced by the electron propagator computed in this paper, there appears one more peak in the single-particle spectrum at very low momenta (Fig. 12).

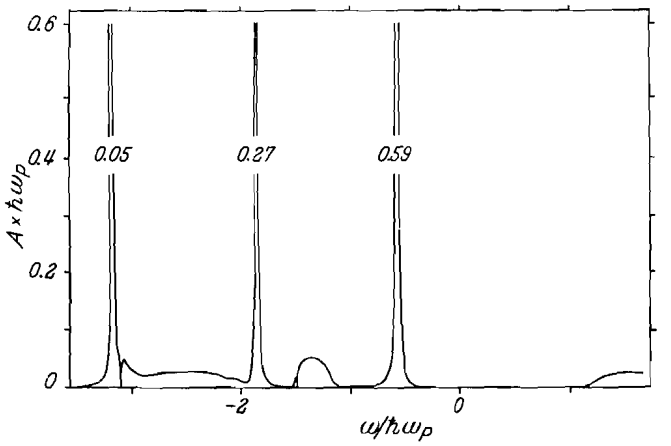

Fig. 12. Typical behaviour of the spectral weight function $A(k, \omega)$ at low momenta according to a second iteration of the Dyson equation ($r_s = 4$, $k = 0.2\, k_F$)

This third peak is a reflexion of the second peak of the first iteration. Its energy differs with considerably more than two times the plasma energy from the quasi-particle peak, and the spectral weight connected to it is much smaller than those connected to the other peaks. In the electron-phonon problem, multiple-phonon processes give no additional structure in the self-energy [17]. However, multiple-plasmon processes do show up in the single-particle spectrum. This difference in behaviour is due to the singular electron-plasmon coupling.

Acknowledgement. The author is grateful to G. Björkman, L. Hedin and S. Lundqvist at the Institute of Theoretical Physics in Göteborg for many discussions and suggestions at various stages of this investigation, and to Profs. J. Krumhansl and J. W. Wilkins for some illuminating discussions.

References

1. Lundqvist, B. I.: Preceding paper. Herafter called part I.
2. Hedin, L.: Phys. Rev. **139**, A 793 (1965).
3. Dubois, D. F.: Ann. Phys. (N. Y.) **7**, 174 (1959); **8**, 24 (1959).
4. McKeeman, W. M., and L. Tesler: Comm. ACM **6**, 315 (1963).
5. Leavenworth, B.: Comm. ACM **3**, 602 (1960).
6. Seitz, F.: Modern theory of solids. New York: McGraw-Hill Book Company Inc. 1940.
7. Daniel, E., and S. H. Vosko: Phys. Rev. **120**, 2141 (1960);
   Kulik, I. O.: Soviet Physics - JETP **13**, 946 (1961).
8. Osaka, Y.: J. Phys. Soc. Japan **18**, 652 (1961);
   Geldart, D. J. W., and S. H. Vosko: J. Phys. Soc. Japan **20**, 20 (1965).
9. Geldart, D. J. W., A. Houghton, and S. H. Vosko: Can. J. Phys. **42**, 1938 (1964).
10. Rice, T. M.: Ann. Phys. (N. Y.) **31**, 100 (1965).
11. Quinn, J. J.: Phys. Rev. **126**, 1453 (1962).
12. Galitskii, V., and A. Migdal: Soviet Physics - JETP **7**, 96 (1958).
13. Engesberg, S.: Phys. Rev. **123**, 1130 (1961).
14. Luttinger, J. M.: Phys. Rev. **119**, 1153 (1960).
15. Schrieffer, J. R.: Theory of superconductivity. New York: W. A. Benjamin Inc. 1964.
16. Bose, S. M., A. Bardasis, A. J. Glick, D. Hone, and P. Longe: Phys. Rev. **155**, 379 (1967).
17. Engelsberg, S., and J. R. Schrieffer: Phys. Rev. **131**, 993 (1963).